JACS
JOURNAL OF THE AMERICAN CHEMICAL SOCIETY
Communication
pubs.acs.org/JACS

Carbene Supported Dimer of Heavier Ketenimine Analogue with P and Si Atoms

Sudipta Roy,[†] Birger Dittrich,*[,∥] Totan Mondal,[‡] Debasis Koley,*[,‡] A. Claudia Stückl,[†] Brigitte Schwederski,[§] Wolfgang Kaim,*[,§] Michael John,[⊥] Suresh Kumar Vasa,[#] Rasmus Linser,[#] and Herbert W. Roesky*[,†]

[†]Institut für Anorganische Chemie, Georg-August-Universität, Tammannstraße 4, 37077 Göttingen, Germany
[∥]Chemistry Department, University of Hamburg, Martin-Luther-King-Platz 6, 20146 Hamburg, Germany
[‡]Department of Chemical Sciences, Indian Institute of Science Education and Research (IISER) Kolkata, Mohanpur 741246, India
[§] Institut für Anorganische Chemie, Universität Stuttgart, Pfaffenwaldring 55, 70569 Stuttgart, Germany
[⊥]Institut für Organische und Biomolekulare Chemie, Georg-August-Universität, Tammannstraße 2, 37077 Göttingen, Germany
[#]Abtl. NMR-basierte Strukturbiologie, Max-Planck-Institut für Biophysikalische Chemie, Am Faßberg 11, 37077 Göttingen, Germany

Supporting Information

ABSTRACT: A cyclic alkyl(amino) carbene (cAAC) stabilized dimer $[(cAAC)Si(P\text{-}Tip)]_2$ (**2**) (Tip = 2,4,6-triisopropylphenyl) is reported. **2** can be considered as a dimer of the heavier ketenimine ($R_2C{=}C{=}N{-}R$) analogue. The dark-red rod-shaped crystals of **2** were synthesized by reduction of the precursor, cAAC-dichlorosilylene-stabilized phosphinidene $(cAAC)SiCl_2{\rightarrow}$P-Tip with sodium napthalenide. The crystals of **2** are storable at room temperature for several months and stable up to 215 °C under an inert atmosphere. X-ray single-crystal diffraction revealed that **2** contains a cyclic nonplanar four-membered SiPSiP ring. Magnetic susceptibility measurements confirmed the singlet spin ground state of **2**. Cyclic voltammetry of **2** showed a quasi-reversible one-electron reduction indicating the formation of the corresponding radical anion $\mathbf{2}^{\bullet-}$, which was further characterized by EPR measurements in solution. The electronic structure and bonding of **2** and $\mathbf{2}^{\bullet-}$ were studied by theoretical calculations. The experimentally obtained data are in good agreement with the calculated values.

Carbenes are shown as efficient ligands in numerous areas of chemistry.[1] In this context, stable N-hetero cyclic carbenes (NHC) are the most extensively utilized ligands due to their early discovery in 1991 and relatively easy available synthesis routes.[1b] NHCs are recognized as strong σ-donors due to the presence of two σ-withdrawing and π-donating nitrogen atoms bonded to the carbene carbon atom. As a result, they are employed as suitable donors for the stabilization of several unstable species such as Si_2,[2a] $(SiCl)_2$,[2a] $SiCl_2$,[2b] SiI^+,[2c] and even some radicals.[2d] NHCs can also stabilize P_2[3a] and P_2O_4 units.[3b] On the contrary, low-coordinate phosphorus−silicon species stabilized by carbenes are only rarely studied until now.[4−6] The very weak π-accepting property of NHCs[7a] can be greatly increased when one of the σ-withdrawing and π-donating nitrogen atoms in NHC is replaced by a σ-donating quaternary carbon atom.[7b] This modified carbene, called the cyclic alkyl(amino) carbene (cAAC), was first reported in 2005.[7c] It has been observed so far that the electronic properties of analogous compounds containing NHC and cAAC are profoundly different.[3a,8] Further reports show that the nature of the bond (coordinate bond vs electron-sharing single bond[9a] and donor−acceptor bond vs double bond)[9b,c] between silicon and carbene carbon can dramatically change depending on the coordination geometry, electron accumulation, and formal oxidation state of the silicon atom.[5,9] NHCs and cAACs are genuinely different from each other, since the HOMO−LUMO energy gap is smaller for the latter one. This often plays a crucial role on the isolation of the final products in silicon chemistry.[2b,10] NHC and cAAC both provide strong σ-donations, while cAAC additionally utilizes its π-acceptance property to synergistically strengthen the $Si{-}C_{cAAC}$ bond.[9c]

Keeping these pivotal differences in mind, cAAC-dichlorosilylene stabilized phosphinidene $(cAAC)SiCl_2{\rightarrow}$P-Tip (**1**) was employed under two-electron reduction to produce (cAAC)Si═P-Tip. This monomeric species could be considered as the heavier ketenimine ($R_2C{=}C{=}N{-}R$) analogue with P and Si atoms instead of N and C atoms, respectively.[6,11] However, a dimer $[(cAAC)Si(P\text{-}Tip)]_2$ (**2**) is isolated instead of the expected monomer (cAAC)Si═P-Tip. Herein, we report on the synthesis, characterization, magnetic susceptibility, CV, and DFT calculations of **2**.

The precursor $(cAAC)SiCl_2{\rightarrow}$P-Tip (**1**)[5] was dissolved in THF, and the resulting dark-blue solution was then cooled to −78 °C. A freshly prepared dark-green THF solution of 2.4 equiv sodium napthalenide ($NaC_{10}H_8$) was separately cooled to 0 °C and added to the flask containing **1**. A dark-purple-red solution was immediately obtained. The temperature of this solution was slowly raised to room temperature over 30 min under vigorous stirring. The stirring was continued for another 3.5 h to obtain a dark-brick-red solution of $[(cAAC)Si(P\text{-}Tip)]_2$ (**2**) (Scheme 1). The solvent was removed *in vacuo* and the residue was extracted with *n*-hexane. The concentrated *n*-hexane solution was stored at

Received: April 3, 2015
Published: April 28, 2015

DOI: 10.1021/jacs.5b03407
J. Am. Chem. Soc. 2015, 137, 6180−6183

Scheme 1. Synthesis Route of $[(cAAC)Si(P\text{-}Tip)]_2$ (2)

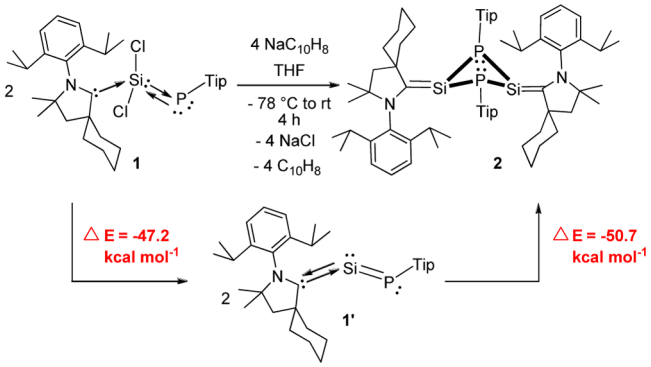

−32 °C for 3 days to obtain dark-red rods of **2** in 61% yield, which were separated by filtration and dried *in vacuo*.

The formation of **2** proceeds via dimerization of the initially formed intermediate species **1′** (Cy-cAAC stabilized heavier analogue of ketenimine; (Cy-cAAC)Si═P-Tip, (**1′**); Scheme 1). This could be attributed to the formation of the dark-purple-red color of the reaction solution at the initial stage. The UV−vis spectrum of the purple-red colored reaction solution was immediately recorded, which showed strong bands at 461 and 534 nm. After 20−30 min this band disappeared and a new band was observed at 524 nm (see SI). The *in situ* formation of the monomeric intermediate (Cy-cAAC)Si═P-Tip (**1′**) was further investigated by detailed NMR measurements in solution (see SI). The immediately recorded ^{31}P NMR spectrum of the dark-purple reaction solution in THF-d_8 shows a sharp highly deshielded singlet (309.6 ppm) flanked by a pair of ^{29}Si satellites (J_{Si-P} = 163 Hz). The ^{29}Si NMR spectrum of the same solution exhibited a doublet at 288.3 ppm (J_{Si-P} = 163 Hz), which is even more downfield shifted, when compared with the so far reported most deshielded ^{29}Si NMR resonance of phosphasilene (267.3 ppm, d, J_{Si-P} = 170.4 Hz).[6] ^{13}C NMR spectrum exhibited a doublet at 242.4 ppm for the $C_{carbene}$. All these data unambiguously prove the *in situ* formation of the monomeric phosphasilene (Cy-cAAC)Si═P-Tip (**1′**) which eventually undergoes dimerization to produce the thermodynamically more stable and isolable compound **2**.

The dark-red crystals of **2** are stable in air for ∼30 min and afterward slowly turn to a colorless solid within the next 30−40 min. Solutions of **2** in *n*-hexane are stable at −32 to 0 °C for several months. The crystals of **2** do not decompose at room temperature for more than two months in an inert atmosphere. **2** melts in the temperature range of 187−188 °C to form a dark-red liquid which decomposes above 215 °C. The NMR spectroscopic analysis of **2** was carried out both in solution and the solid phase (see SI). ^{31}P NMR spectrum of **2** in THF-d_8 solution exhibits a singlet at −113.4 ppm flanked by a pair of ^{29}Si satellites (J_{Si-P} = 44 Hz) which is downfield shifted when compared with that of the precursor **1** (−123.0 ppm; J_{Si-P} = 198 Hz). The ^{29}Si NMR spectrum of **2** exhibits a triplet at 37.1 ppm (J_{Si-P} = 44 Hz) in solution. ^{13}C NMR spectrum of **2** shows a resonance at 203.5 ppm for $C_{carbene}$, which is slightly upfield shifted when compared to that of **1** (208.1 ppm). ^{31}P, ^{29}Si, and ^{13}C CPMAS spectra of **1** and **2** in the solid-state (Figures S1−S3) gave similar isotropic chemical shift values as in solution. In solid-state ^{31}P, ^{29}Si, and ^{13}C chemical shift values of **2** are −110.5, 35.3/35.1, and 201.9/198.9 (C_{cAAC}) ppm, respectively. These values follow the similar trend with theoretical calculation (see SI). The UV−vis spectrum of **2** was recorded in *n*-hexane, which shows broad absorption bands (455, 524 nm; see SI for details).

Compound **2** crystallizes in the monoclinic space group $P2_1/n$. The molecular structure of **2** is displayed in Figure 1, which

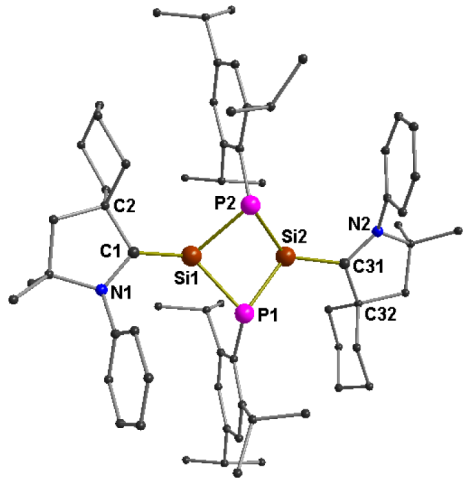

Figure 1. Crystal structure of **2**. Hydrogen atoms and selected isopropyl groups of carbenes are omitted for clarity. Selected experimental [calculated at the M06-2X/SVP level of theory] bond lengths [Å], and angles [°]. Si1−C1 1.812(2) [1.816], Si2−C31 1.812(2) [1.819], C1−N1 1.389(3) [1.365], C31−N2 1.390(3) [1.364], P1−Si1 2.2655(7) [2.279], P1−Si2 2.2953(8) [2.310], P2−Si2 2.2691(8) [2.281], P2−Si1 2.2898(8) [2.312]; Si1−P1−Si2 79.21(3) [79.3], Si2−P2−Si1 79.25(3) [79.3], P1−Si1−P2 86.79(3) [86.3], P2−Si2−P1 86.57(3) [86.2], N1−C1−C2 108.89(17) [109.3], N2−C31−C32 108.67(17) [109.3], Si1−P1−Si2-P2 38.83(4) [39.3].

shows the formation of a cyclic nonplanar four-membered Si_2P_2 ring supporting the formation of (Cy-cAAC)Si═P-Tip as an intermediate species (**1′**) which finally underwent a [2 + 2]-cycloaddition reaction across the two Si═P bonds. Each phosphorus atom in **2** is bound to a Tip group and each silicon atom to a carbene (Cy-cAAC). The P-Tip groups are oriented in *cis* conformation with respect to the Si_2P_2 ring. The aromatic rings of Tip groups are arranged perpendicular to the Si_2P_2 ring, while the five-membered carbene rings of Cy-cAAC are parallel to the average plane of the Si_2P_2 ring. Both the silicon (∼0.4 Å above $P1C_{cAAC}P2$ plane) and phosphorus (∼0.4 Å above $Si1C_{Tip}Si2$ plane) atoms adopt a trigonal pyramidal geometry, while the carbene carbon atoms adopt a near-planar geometry (∼0.16 Å above N1Si1C2/N2Si2C32 planes). In comparison, the silicon and phosphorus atoms of precursor **1** adopt distorted-tetrahedral and bent geometries, respectively. The Si−P/Si−C/C−N bond distances in **1** and **2** are 2.1225(9)/1.945(2)/1.308(3) and 2.2655(7)−2.2953(8) /1.812(2)/1.389(3)−1.390(3) Å, respectively. The bond parameters of **2** suggest that the bond between the carbene carbon atom and the silicon atom is an electron-sharing bond (∼1.812 Å), whereas, that in **1** is a coordinate bond (C→Si). Thus, the valence bond electron count leads to the conclusion that the intramolecular Si1−Si2 and $C_{cAAC}-C_{cAAC}$ distances are ∼2.9 and ∼6.5 Å, respectively. The shortest intermolecular $C_{cAAC}-C_{cAAC}$, Si−Si and $Si-C_{cAAC}$ distances are ∼9.2, 11.2, and 10.1 Å, respectively.

Optimization (at M06-2X/167 SVP level of theory) of both the singlet and triplet states of **2** showed that the former is the electronic ground state with an energy difference ($\Delta E_{S\rightarrow T}$) of 14.2 kcal mol^{-1}. The optimized geometrical parameters of the singlet state are in good agreement with the X-ray crystal

DOI: 10.1021/jacs.5b03407
J. Am. Chem. Soc. 2015, 137, 6180−6183

structure as seen from the alignment and superposition of the geometries (Figure S7, Table S5). The Si1−C1/Si2−C31 bonds in **2** are significantly shorter (1.816/1.819 Å) than in precursor **1** (1.969 Å) due to the stronger π-bond as visualized in the occupied frontier orbitals (KS-HOMO and KS-HOMO−1, Figure 2) with respect to a donor−acceptor (C: → Si) type

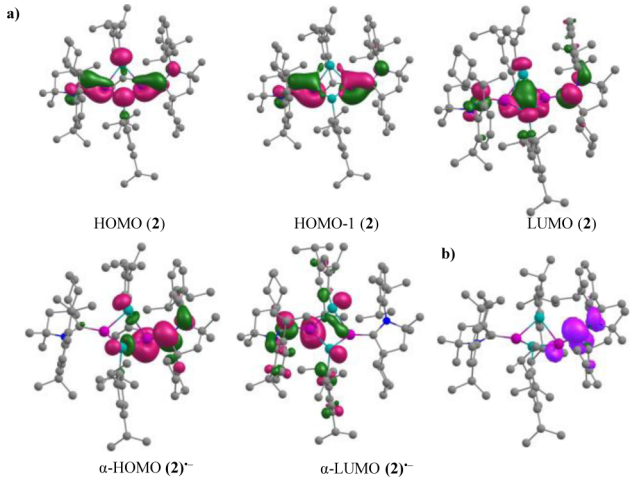

Figure 2. (a) KS-MOs of **2** and **2**$^{\bullet-}$ (isosurface = 0.04 au) and (b) Mulliken spin density plots for **2**$^{\bullet-}$ (isosurface = 0.003 au).

interaction inherent in monomer **1**.[5] Formation of intermediate **1**′ [11] from the precursor **1**, is highly favorable ($\Delta E_{1\rightarrow 1'}$ = −47.2 kcal mol^{-1}), which then readily dimerizes to the more stable compound **2** ($\Delta E_{1'\rightarrow 2}$ = −50.7 kcal mol^{-1}). NBO population analysis of **1**′ exhibits a single σ-type natural orbital for the $C_{carbene}$−Si with electron occupancy of 1.936 e which is strongly polarized toward the $C_{carbene}$ atom (∼80%). NBO also locate the lone pair occupancies of 1.781 and 1.939 e at Si and P atoms, respectively. This finding indicates the donor−acceptor character of $C_{carbene}$−Si bond (Figure S8). From NBO analysis of **2**, C1−N1 and C1−C2 show single bond occupancies of 1.978 and 1.959 e, respectively, while the Si1−C1/Si2−C31 bonds exhibit double bond character with σ and π occupancies of 1.912 and 1.857 e. The Si1−C1/Si2−C31 σ-bonded electron density is polarized toward C1/C31 centers (C: ∼70%), while the π-bonded electron density is equally contributed (C: ∼52%) between the bonding partners as represented by the natural localized molecular orbitals plot for C−Si bonds (Figure S8). Wiberg bond indices calculated for Si−C bonds are 1.21, 0.88, and 0.63 for **2**, **1**′, and **1** respectively. These values are supported from the reported NBO and molecular orbital analysis. The bonding scenario of Si1−C1 bond was further elucidated by QTAIM calculations.[11] The important topological parameters at the (3,-1) bond critical points are given in Table S6. The electron density [ρ(r)] at the BCP of C1−N1 [0.307], C1−C2 [0.238] and Si1−C1 [0.113] bonds along with the respective Laplacian [$\nabla^2\rho$(r); −0.767, −0.557, and +0.398] indicates covalent interaction in former two bonds and closed-shell interaction in last one (Si1−C1; see Table S6), since polarization toward C1 center allows deviation from covalent character. On the other hand the calculated ellipticity for Si1−C1 (ε_{BCP} = 0.39) is much higher than the C:→Si (ε_{BCP} = 0.04) in precursor **1**, indicating its covalent nature compared to the closed-shell interaction in the monomeric fragment. The delocalization indices (DI) value for Si1−C1 (0.95) is close to the Si═C (1.17) double bond in $H_2Si{=}CH_2$.[11] TDDFT treatment of **2** (B3LYP/TZVP//M06-2X/SVP) provides three low energy absorption peaks at 433, 456, and 569 nm (f = 0.269, 0.047, and 0.073) primarily designating the $\pi_{Si1-C1/Si2-C31} \rightarrow \pi^*_{Si1-C1/Si2-C31}$ excitation. In case of transient species **1**′ absorptions at 429 and 461 nm (f = 0.091 and 0.032) are characterized with $LP_{Si} \rightarrow \pi^*_{Si-P}$ excitations indicating the weakening of the Si−P bond before collapsing to the dimeric structure.

The temperature-dependent magnetic susceptibility measurements confirm that the spin ground state of **2** is S = 0, which agrees with the theoretical predictions. Compound **2** was further studied by CV in a THF solution containing 0.1 M [n-Bu_4N]ClO_4 as an electrolyte. The CV shows a one-electron quasi-reversible process at $E_{1/2}$ = −0.87 V against $Cp^*_2Fe/Cp^*_2Fe^+$, suggesting the formation of the radical anion **2**$^{\bullet-}$ (Figure 3, right). One-electron reduction of **2** leads to radical anion **2**$^{\bullet-}$ accompanying an energy of 19.2 kcal mol^{-1} (0.83 eV) that can be readily accessible under ambient conditions.

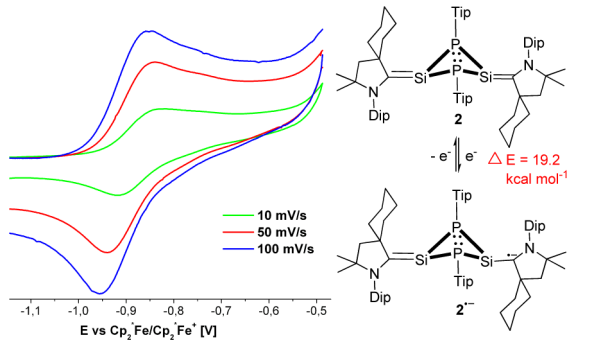

Figure 3. Section of cyclic voltammogram of THF solution of **2** at indicated scan rates, containing 0.1 M [n-Bu_4N]ClO_4 as electrolyte.

The X-band EPR spectrum of *in situ* generated **2**$^{\bullet-}$ (a typical S = 1/2 species) in toluene solution at 285 K consists of 12 well-resolved lines of equal intensity. The splitting pattern as reproduced by simulation (Figure 4, top) shows a doublet of

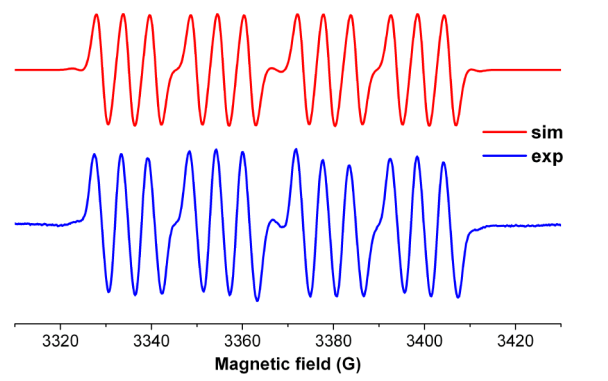

Figure 4. EPR spectra of compound **2**$^{\bullet-}$ (simulated; red) and (experimental; blue) at 285 K.

doublets, each component split further into three equidistant lines. The latter splitting must be assigned to the coupling of electron spin with one ^{14}N nucleus (I = 1) at 5.9 G, i.e., in the typical range for cAAC radicals.[9a,e] The two larger doublet hyperfine splittings at 44.1 and 20.6 G are attributed to two inequivalent ^{31}P nuclei (I = 1/2). EPR coupling constants of ^{31}P are frequently large due to the high nuclear magnetic moment, not necessarily reflecting very large spin densities. Nevertheless,

DOI: 10.1021/jacs.5b03407
J. Am. Chem. Soc. 2015, 137, 6180−6183

the notable deviation of the g factor (2.0062) from the free electron value of 2.0023 can be traced to the higher spin orbit coupling constant of the second-row element phosphorus in contrast to nitrogen. The inequivalence of the two ^{31}P nuclei in the EPR experiment agrees with the calculated difference in orientation of the P-involving bonds with respect to the mainly spin-bearing p(z) orbital at the carbene carbon center. Accordingly, a ^{29}Si satellite isotope coupling (I = 1/2, 4.7% nat. abundance) with a typical[9a,e] value of about 11 G is also observed.

The reduction results in an increase of electron density in the LUMO of **2**, comprising the C1−N1/C31−N2 bonds (Figure 2). Obviously, the C1−N1/C31−N2 bond distances are elongated in $\mathbf{2}^{\bullet-}$ (1.365/1.364 in **2** vs 1.405/1.413 in $\mathbf{2}^{\bullet-}$). To mention another important geometrical change, the Si−C bond lengths become unsymmetrical (Si1−C1/Si2−C31 = 1.778/1.896; Table S5) in $\mathbf{2}^{\bullet-}$, as the radical resides on C31 atom in α-HOMO (Figure 2). Similarly, NBO captures an analogous electronic environment with higher σ and π bond occupancies (1.948 and 1.892 e) in Si1−C1 bond and single-bond occupancy (1.949 e) for Si2−C31, with an additional lone pair character at C31 atom. Further support has been obtained from valence-shell charge concentrations plots calculated from QTAIM calculation clearly designating the localization of the radical at carbene carbon (Figure S9). The Mulliken spin-density plots of $\mathbf{2}^{\bullet-}$ at the UM06-2X/TZVP//UM06-2X/SVP level are plotted in Figure 2. The calculated spin density points unambiguously shows the position of the unpaired electron at the carbene carbon (C31), with a minor contribution from neighboring N2 and Si2 atoms (Tables S7−8).

In conclusion, we have synthesized an unprecedented dimeric heavier analogue of ketenimine with phosphorus and silicon atoms $[(cAAC)Si(P\text{-}Tip)]_2$ (**2**). NMR studies and theoretical calculations show that **2** forms via dimerization of *in situ* generated monomer (cAAC)Si═P-Tip (**1′**). **2** contains a cyclic nonplanar four-membered Si_2P_2 ring with two cAAC=Si units. **2** was isolated as dark-red rods which are stable for months under an inert atmosphere. **2** possesses an S = 0 spin ground state. Theoretical calculations showed that the singlet ground state of **2** is 14.2 kcal mol^{-1} lower in energy than that of the triplet state. Analysis of bond parameters suggests a covalent double-bond character of the cAAC=Si bond of **2**, while a closed-shell interaction is preferred in precursor **1**. The redox properties of **2** have been studied by CV which suggest the formation of the radical anion $\mathbf{2}^{\bullet-}$. The formation of $\mathbf{2}^{\bullet-}$ was further confirmed by EPR spectroscopy. Theoretical calculations and simulation of EPR spectrum showed that the radical electron resides on the carbene carbon atom and couples with one ^{14}N and two ^{31}P nuclei of $\mathbf{2}^{\bullet-}$.

■ ASSOCIATED CONTENT

Supporting Information

Synthesis of **2**, NMR, magnetic measurements, UV−vis, CV, crystal structure determination, EPR of $\mathbf{2}^{\bullet-}$, and theoretical details. The Supporting Information is available free of charge on the ACS Publications website at DOI: 10.1021/jacs.5b03407.

■ AUTHOR INFORMATION

Corresponding Authors

*hroesky@gwdg.de
*koley@iiserkol.ac.in
*birger.dittrich@chemie.uni-hamburg.de
*kaim@iac.uni-stuttgart.de

Notes

The authors declare no competing financial interest.

■ ACKNOWLEDGMENTS

H.W.R. thanks Deutsche Forschungsgemeinschaft (DFG RO 224/60-I) and D.K. to IISER-Kolkata CSIR project fund (01(2770)/13/EMR-II) for financial support. We thank Dr. K. C. Mondal for scientific suggestions, Dr. S. Demeshko for magnetic susceptibility measurements, Mr. J. Meyer for CV measurements, and Prof. S. Schneider for his UV−vis spectrophotometer facility. R.L. thanks Verband der Chemischen Industrie for a Liebig fellowship, and T. M. acknowledges CSIR for SRF fellowship. Dedicated to Wacker Chemie on the occasion of the 100th anniversary.

■ REFERENCES

(1) (a) Hopkinson, M. N.; Richter, C.; Schedler, M.; Glorius, F. *Nature* **2014**, *510*, 485. (b) Arduengo, A. J., III; Harlow, R. L.; Kline, M. *J. Am. Chem. Soc.* **1991**, *113*, 361.

(2) (a) Wang, Y.; Xie, Y.; Wei, P.; King, R. B.; Schaefer, H. F., III; Schleyer, P. v. R.; Robinson, G. H. *Science* **2008**, *321*, 1069. (b) Ghadwal, R. S.; Roesky, H. W.; Merkel, S.; Henn, J.; Stalke, D. *Angew. Chem., Int. Ed.* **2009**, *48*, 5683; *Angew. Chem.* **2009**, *121*, 5793. (c) Filippou, A. C.; Lebedev, Y. N.; Chernov, O.; Straßmann, M.; Schnakenburg, G. *Angew. Chem., Int. Ed.* **2013**, *52*, 6974; *Angew. Chem.* **2013**, *125*, 7112. (d) Nozawa, T.; Ichinohe, M.; Sekiguchi, A. *J. Am. Chem. Soc.* **2012**, *134*, 5540.

(3) (a) Wang, Y.; Xie, Y.; Wie, P.; King, R. B.; Schaefer, H. F., III; Schleyer, P. v. R.; Robinson, G. H. *J. Am. Chem. Soc.* **2008**, *130*, 14970. (b) Wang, Y.; Xie, Y.; Wei, P.; Schaefer, H. F., III; Schleyer, P. v. R.; Robinson, G. H. *J. Am. Chem. Soc.* **2013**, *135*, 19139.

(4) (a) Hansen, K.; Szilvási, T.; Blom, B.; Inoue, S.; Epping, J.; Dries, M. *J. Am. Chem. Soc.* **2013**, *135*, 11795. (b) Hansen, K.; Szilvasi, T.; Blom, B.; Irran, E.; Driess, M. *Chem.—Eur. J.* **2014**, *20*, 1947. (c) Back, O.; Henry-Ellinger, M.; Martin, C. D.; Martin, D.; Bertrand, G. *Angew. Chem., Int. Ed.* **2013**, *52*, 2939; *Angew. Chem.* **2013**, *125*, 3011.

(5) Roy, S.; Stollberg, P.; Herbst-Irmer, R.; Stalke, D.; Andrada, D. M.; Frenking, G.; Roesky, H. W. *J. Am. Chem. Soc.* **2015**, *137*, 150.

(6) Geiß, D.; Arz, M. I.; Straßmann, M.; Schnakenburg, G.; Filippou, A. C. *Angew. Chem., Int. Ed.* **2015**, *54*, 2739; *Angew. Chem.* **2015**, *127*, 2777.

(7) (a) Tonner, R.; Heydenrych, G.; Frenking, G. *Chem.—Asian J.* **2007**, *2*, 1555. (b) Martin, D.; Canac, Y.; Lavallo, V.; Bertrand, G. *J. Am. Chem. Soc.* **2014**, *136*, 5023. (c) Lavallo, V.; Canac, Y.; Präsang, C.; Donnadieu, B.; Bertrand, G. *Angew. Chem., Int. Ed.* **2005**, *44*, 5705; *Angew. Chem.* **2005**, *117*, 5851.

(8) Back, O.; Donnadieu, B.; Parameswaran, P.; Frenking, G.; Bertrand, G. *Nat. Chem.* **2010**, *2*, 369.

(9) (a) Mondal, K. C.; Roesky, H. W.; Stückl, A. C.; Ihret, F.; Kaim, W.; Dittrich, B.; Maity, B.; Koley, D. *Angew. Chem., Int. Ed.* **2013**, *52*, 11804; *Angew. Chem.* **2013**, *125*, 12020. (b) Mondal, K. C.; Roesky, H. W.; Schwarzer, M. C.; Frenking, G.; Tkach, I.; Wolf, H.; Kratzert, D.; Herbst-Irmer, R.; Niepötter, B.; Stalke, D. *Angew. Chem., Int. Ed.* **2013**, *52*, 1801; *Angew. Chem.* **2013**, *125*, 1845. (c) Mondal, K. C.; Roesky, H. W.; Schwarzer, M. C.; Frenking, G.; Niepötter, B.; Wolf, H.; Herbst-Irmer, R.; Stalke, D. *Angew. Chem., Int. Ed.* **2013**, *52*, 2963; *Angew. Chem.* **2013**, *125*, 3036. (d) Roy, S.; Mondal, K. C.; Krause, L.; Stollberg, P.; Herbst-Irmer, R.; Stalke, D.; Meyer, J.; Stückl, A. C.; Maity, B.; Koley, D.; Vasa, S. K.; Xiang, S. Q.; Linser, R.; Roesky, H. W. *J. Am. Chem. Soc.* **2014**, *136*, 16776. (e) Roy, R.; Stückl, A. C.; Demeshko, S.; Dittrich, B.; Meyer, J.; Maity, B.; Koley, D.; Schwederski, B.; Kaim, W.; Roesky, H. W. *J. Am. Chem. Soc.* **2015**, *137*, 4670.

(10) Mondal, K. C.; Dittrich, B.; Maity, B.; Koley, D.; Roesky, H. W. *J. Am. Chem. Soc.* **2014**, *136*, 9568.

(11) See SI.

DOI: 10.1021/jacs.5b03407
J. Am. Chem. Soc. 2015, 137, 6180−6183